University of Groningen

Water-based alkyl ketene dimer ink for user-friendly patterning in paper microfluidics

Hamidon, Nurul; Hong, Yumiao; Salentijn, Gert; Verpoorte, Elisabeth

IMPORTANT NOTE: You are advised to consult the publisher's version (publisher's PDF) if you wish to cite from it. Please check the document version below.

Document Version
Publisher's PDF, also known as Version of record

[Link to publication in University of Groningen/UMCG research database](#)

Water-based alkyl ketene dimer ink for user-friendly patterning in paper microfluidics

Nurul Nadiah Hamidon [a, b], Yumiao Hong [a], Gert IJ. Salentijn [a, c], Elisabeth Verpoorte [a, *]

[a] Pharmaceutical Analysis, Groningen Research Institute of Pharmacy, University of Groningen, 9700 AD Groningen, The Netherlands
[b] Faculty of Industrial Sciences & Technology, Universiti Malaysia Pahang, 26300 Kuantan, Malaysia
[c] TI-COAST, Science Park 904, 1098 XH Amsterdam, The Netherlands

HIGHLIGHTS

- Hydrophobic barriers were introduced on paper by using water-based AKD ink.
- AKD barrier wettability was controlled by varying the alcohol content in eluent.
- Aqueous reagents can be stored individually in AKD-patterned storage chamber.
- Hand-drawn AKD barriers improved the elution and signal of analytes in PSI-MS analysis.

GRAPHICAL ABSTRACT
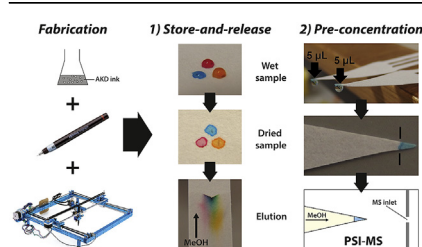
ABSTRACT

We propose the use of water-based alkyl ketene dimer (AKD) ink for fast and user-friendly patterning of paper microfluidic devices either manually or using an inexpensive XY-plotter. The ink was produced by dissolving hydrophobic AKD in chloroform and emulsifying the solution in water. The emulsification was performed in a warm water bath, which led to an increased rate of the evaporation of chloroform. Subsequent cooling led to the final product, an aqueous suspension of fine AKD particles. The effects of surfactant and AKD concentrations, emulsification procedure, and cooling approach on final ink properties are presented, along with an optimized protocol for its formulation. This hydrophobic agent was applied onto paper using a plotter pen, after which the paper was heated to allow spreading of AKD molecules and chemical bonding with cellulose. A paper surface patterned with the ink (10 g L^{-1} AKD) yielded a contact angle of $135.6°$ for water. Unlike organic solvent-based solutions of AKD, this AKD ink does not require a fume hood for its use. Moreover, it is compatible with plastic patterning tools, due to the effective removal of chloroform in the production process to less than 2% of the total volume. Furthermore, this water-based ink is easy to prepare and use. Finally, the AKD ink can also be used for the fabrication of so-called selectively permeable barriers for use in paper microfluidic networks. These are barriers that stop the flow of water through paper, but are permeable to solvents with lower surface energies. We applied the AKD ink to confine and preconcentrate sample on paper, and demonstrated the use of this approach to achieve higher detection sensitivities in paper spray ionization-mass spectrometry (PSI-MS). Our patterning approach can be employed outside of the analytical lab or machine workshop for fast prototyping and small-scale production of paper-based analytical tools, for use in limited-resource labs or in the field.

* Corresponding author. Antonius Deusinglaan 1, P.O. Box 196, 9700 AD, Groningen, The Netherlands.
  E-mail address: E.M.J.Verpoorte@rug.nl (E. Verpoorte).

1. Introduction

Paper is a very cheap and readily available material for making microfluidic devices for chemical assays, and offers several advantages compared to other materials. One important advantage is passive fluid transport due to capillary action [1–3]. Dissolved reagents and sample can be delivered with no external effort to a particular region of a paper device for chemical reaction or other processing, such as analyte separation [4,5]. Furthermore, the porosity of paper reduces the need to chemically or physically immobilize reagents, because reagents can be retained in the pores [6]. The nearly-white background of paper makes it easy for the user to observe colorimetric reactions by eye [4,7,8]. Finally, multiple components, such as reaction vessels [9], mixing structures [10,11], or separation chambers [12–14], can be patterned in an integrated manner onto a piece of paper to carry out the desired physical, chemical and biological processing. This makes paper an attractive option for, among other things, on-site environmental testing and point-of-care diagnostics, both of which are performed outside of well-equipped centralized laboratories in limited-resource settings [15–20].

To control liquid flows in a paper microfluidic device, barriers can be introduced, commonly by patterning the paper with hydrophobic substances to form chambers and channels [4,21–23]. Barriers can also be formed inside a channel by patterning dissolvable [24,25] or permanent flow obstacles [26] to alter flow velocity.

The process of patterning these "simple and cheap" devices is not always simple and cheap, however. Patterning agents might incorporate dangerous, volatile solvents that need to be handled in a fume hood, or can damage or shorten the lifetime of plastic patterning tools [21,27–29]. Channels can be produced in paper either by adding or removing hydrophobic agent on paper; the approach taken will influence the complexity of the fabrication process. Applying hydrophobic agent to the entire paper substrate and selectively removing it afterwards to create channels (*e.g.* by spraying toluene [30] or exposure to oxygen plasma [23]) is often more cumbersome than directly patterning paper with hydrophobic agents using printers or crayons [31].

To address these issues, the current trend is to pattern paper using a specialized, commercially available inkjet printer or a solid ink (wax) printer [22,32]. These printers offer good resolution and allow fast prototyping. Nonetheless, this option is less feasible when cost is a critical issue or when the research is still in the exploration phase.

Since paper devices are well-suited for use in limited-resource settings, it would be of additional benefit to be able to modify device designs in these settings to accommodate local conditions. For instance, differences in humidity and temperature affect sample elution through the device, and thus device performance. However, these effects could be compensated for by making changes to the dimensions of features such as solvent reservoirs. Once a design has been modified, it is preferential to also have the device manufactured locally, to keep production costs low and production times short.

This work aims to develop a water-based ink containing a hydrophobic agent for fast, user-friendly paper microfluidic patterning using a manual approach or an inexpensive XY-plotter. We chose to work with alkyl ketene dimer (AKD), a commonly used substance in the paper industry to adjust the hydrophobicity of paper products. AKD is made from natural fatty acids (14–22 carbons) and forms chemical bonds with hydroxyl groups in cellulose upon heating [26,33]. This means that it binds to the paper more strongly than wax or other types of agents that rely solely on physical adsorption. While wax works to block liquid wicking by filling or clogging the porous cellulose network, AKD treatment simply makes this network more hydrophobic. This allows the continued passage of liquids having compatible surface energies, but blocking those liquids whose surface energies are mismatched with AKD.

AKD is commercially available as solid flakes or as an emulsion. The shelf life of an AKD emulsion is typically between several weeks and 3 months [34]. The reaction site for hydroxyl groups on AKD can be hydrolysed, converting it into a ketone [35]. This slow process is undesirable, as the ketone form of AKD can no longer bind covalently to cellulose. Therefore, simple, on-site emulsification of AKD is recommended when AKD consumption is low, such as in the case of explorative laboratory research or small-scale production of paper microfluidic devices.

In this report, we demonstrate an easy way to produce an AKD suspension using standard laboratory instrumentation. Furthermore, we show that this AKD ink can be used in conjunction with different patterning strategies, and can be applied to make selectively permeable valves [26]. These are then employed for on-paper preconcentration in a paper spray ionization (PSI) experiment with mass spectrometric (MS) detection [36].

2. Materials and methods

2.1. Chemicals, disposables and equipment

Alkyl ketene dimer (AKD, 22-carbon chain, melting point ca. 65 °C, courtesy of Ashland Inc., Finland), trimethyl(tetradecyl) ammonium bromide (TTAB, Sigma Aldrich, India), Tween 20 (T20, Sigma Aldrich, USA), chloroform (Biosolve B.V., The Netherlands), water (demineralized) and a magnetic stirrer with hotplate (Velp Scientifica, Italy) were used to produce the ink. Methanol-water solutions were prepared from HPLC-grade methanol (BioSolve B.V., The Netherlands) and demineralized water. Solutions ranging from 0% to 100% methanol (v/v) were used for the elution of consumer-grade food dyes deposited on the paper. Blue (E131, Bharco Foods, Netherlands), red (E122, PT. Gunacipta Multirasa, Indonesia), and yellow (E102, PT. Gunacipta Multirasa, Indonesia) food dyes purchased from local food stores were used.

Grade 1 Whatman cellulose chromatography paper (GE Healthcare Life Sciences, China) was used as the paper-microfluidic substrate. Patterning was conducted in one of three ways. For automated patterning, an XY-plotter (V2.0, Makeblock, China) and refillable plotter pen (Isograph pen, 0.6 mm nib, Rotring, Germany) were used. Manual patterning was possible using either the Rotring plotter pen or a do-it-yourself (DIY) pen made of a disposable surgical syringe (ink reservoir) and needle (BD Microlance 3, 0.3 mm outer diameter, Becton, Dickinson and Company, Ireland). The AKD-patterned paper was heated in an oven (OMT, Sanyo Gallenkamp, Loughborough, U.K.). A microscope (Leica S8 APO, Germany), camera (Canon EOS 700D, Japan) mounted on the microscope, and ruler were used to measure the dimensions of the AKD patterns with ImageJ software.

2.2. Optimization of AKD ink formulation

The formulation of ink involves two steps: (i) the emulsification of a chloroform solution of AKD in water, and (ii) the cooling of the mixture (Fig. 1A). The emulsification step was adapted from the work by Missoum et al. [37]. Emulsions were formed by mixing (with magnetic stirring) the oil phase (1 mL of a chloroform solution containing AKD and surfactant) with 10 mL of water in a conical flask placed in a 60 °C water bath. Chloroform evaporates gradually during this step due to the heating. The emulsion was then cooled down to 20 °C. The final product is an aqueous
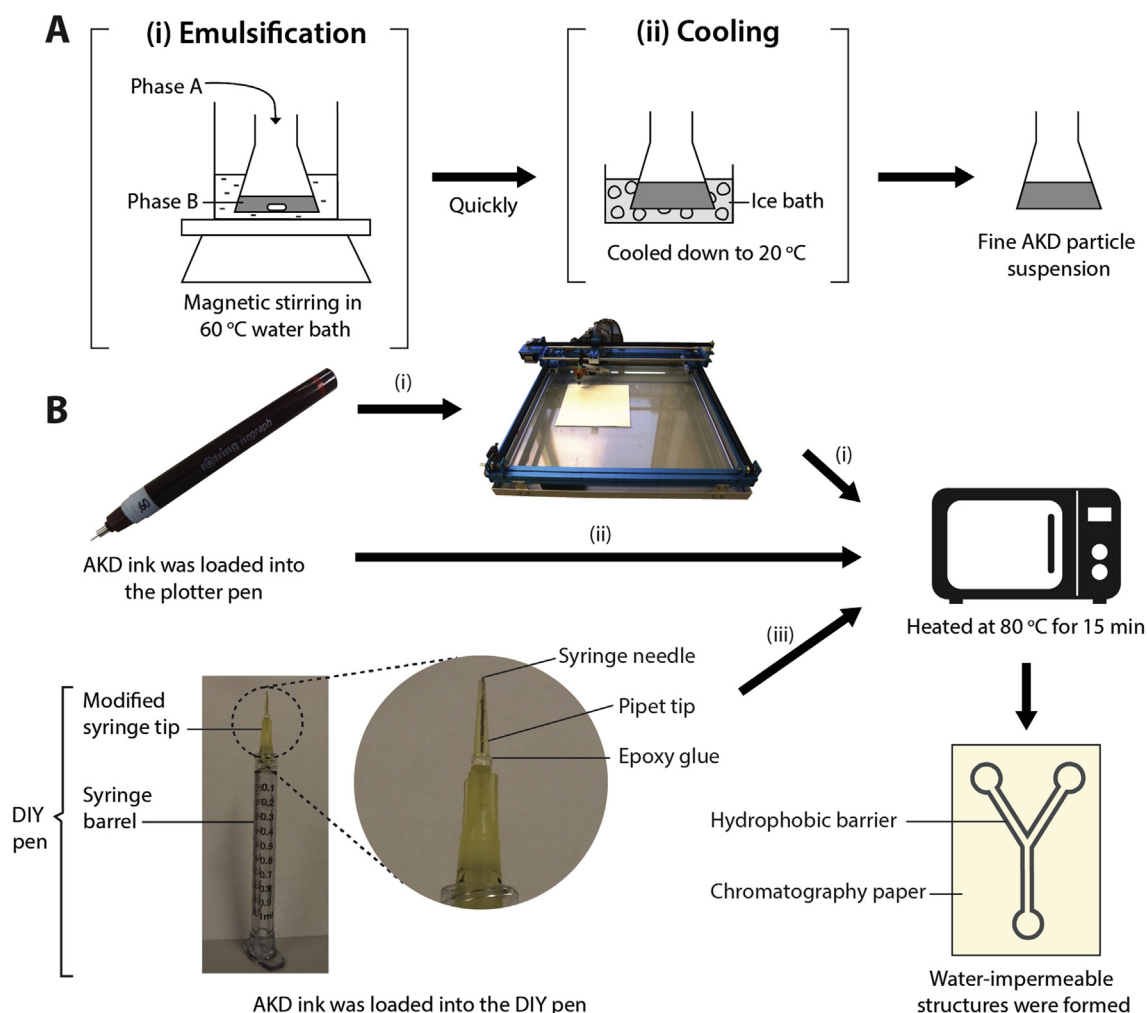
Fig. 1. (A) The general process of producing AKD ink involved two steps: (i) the emulsification of a chloroform solution of AKD in water and (ii) the cooling of the mixture. (B) The patterning of paper was performed in one of three ways: (i) a plotter pen in combination with the XY-plotter (automated); (ii) a plotter pen (manual; with or without a stencil); (iii) DIY pen (manual; with stencil).

suspension of fine AKD particles.

To achieve a stable suspension with small particles of relatively uniform size, the effect of four parameters on AKD particle size in the suspension was investigated: (i) surfactant addition, (ii) route of emulsification, (iii) cooling approach and (iv) AKD concentration. Furthermore, since it is important to remove as much of the chloroform as possible from the final product, the influence of the temperature of the water bath during the emulsification step was also investigated.

Two surfactants were tested, namely T20 and TTAB. Both surfactants were tested at three different concentrations, expressed in terms of their critical micelle concentrations (CMC; $CMC_{T20} = 0.06$ g L^{-1}; $CMC_{TTAB} = 1.51$ g L^{-1}), namely twofold (2x), tenfold (10x) and twentyfold (20x) the respective CMC. The need for a surfactant was also verified in an emulsification experiment in which no added surfactant was used. After selecting the best surfactant type and concentration, the emulsification route was varied by changing the order of addition (water phase to oil phase or vice versa) as well as the manner of combining the phases in the flask (adding a phase all at once or in aliquots). Subsequently, three approaches for the cooling step were tested (slow cooling at room temperature; faster cooling by means of an ice bath; or freezer at −18 °C). Then, experiments using varying concentrations of AKD

in the oil phase (5–10 g L^{-1}) were performed. All experiments and procedures with chloroform were carried out in a fume hood.

The experimental conditions for the optimization of each of the four parameters involved in the preparation of aqueous AKD-particle suspensions (inks) are summarised in Table S1 of the Electronic Supplementary Information (ESI). Three suspensions were produced for each set of conditions. For each suspension, a microscope slide was prepared. Three images were acquired from different locations on each of the microscope slides using a microscope and a digital camera (the area analysed was 451.95 × 337.66 μm per image). ImageJ was used to analyse the size of particles in the suspension [38]. The data were then pooled together (n = 3 × 3) to create a scatter plot and violin plot for each tested set of conditions.

Finally, the optimized protocol for the formulation of aqueous AKD suspensions for our ink application, derived from the optimization of the four parameters above, was used in conjunction with different water bath temperatures (room temperature, 60 °C, and 70 °C). We looked at the transparency of the emulsions in all cases to determine whether chloroform removal had been effective or not. Chloroform and water produce a translucent emulsion. When the chloroform content is below 2% (v/v), it becomes transparent again (see ESI Fig. S1).

2.3. Patterning of paper

The hydrophobic structures were formed on paper by loading the ink (10 g L^{-1} AKD) into the refillable plotter pen or DIY pen, and using the pen to draw the desired structures on chromatography paper either mechanically (XY-plotter; Fig. 1B-i) or manually (Fig. 1B-ii). The ink was allowed to air-dry, after which the paper was heated in an oven at 80 °C for 15 min to melt and spread the AKD, and bond it with the cellulose.

For patterning using the XY-plotter, Inkscape open-source software was used to design the structures, which were then converted into a Gcode (coordinates file) using the *Gcodetools* extension. The generated Gcode was submitted to the plotter software (*XYremote*) to control the movement of the plotter pen when drawing on the chromatography paper. The settings used for drawing with the XY-plotter can be found in ESI Table S2 and the setup in ESI Fig. S2.

The suspension was homogenized by shaking prior to filling the plotter pen. The pen was then shaken horizontally. The nib of the plotter pen was rinsed thoroughly with water after use. If clogging occurred, the nib was immersed in methanol for 30 min and then rinsed with water.

2.4. DIY tool for patterning using AKD ink

To demonstrate the versatility of the AKD ink for patterning, a DIY pen was made as a tool to apply it on paper (Fig. 1B-iii). This DIY pen was constructed by attaching a modified syringe needle to a surgical syringe barrel. The needle was cut to a length of approximately 1 cm. A 20-μL pipette tip was then slipped over the needle and onto the plastic casing of the syringe needle. The end of the pipette tip was cut to a length that allowed approximately 1 mm of syringe needle to protrude from it. Once slipped over the needle, the pipette tip was glued to the needle tip with epoxy glue and left overnight. The pipette tip was included to make the syringe tip more rigid and manageable for manually drawing patterns on paper.

The AKD ink was homogenized by shaking before a volume of 500 μL was loaded into the syringe barrel of the DIY tool. Using 3D-printed stencils, patterns were hand-drawn on paper with the DIY pen. Unlike the plotter pen, the DIY pen was not shaken prior to use, nor did it clog.

2.5. Evaluation of produced patterns

A number of patterns and shapes were drawn manually with the plotter pen (with and without stencils) and DIY pen (with stencils), and with the XY-plotter using the plotter pen. The structures obtained using these approaches were then compared.

The quality of the produced patterns was evaluated in terms of line thickness and uniformity by taking pictures of the drawn lines under a microscope. As AKD patterns on paper are colourless, the paper was wet with water to reveal them. A ruler was included as an internal reference in the images for the measurement, and the captured images were analysed using ImageJ software.

To check the solvent permeability of the AKD patterns, closed squares of 11 × 6 mm (no infill) were drawn with AKD ink. Methanol solution (0, 25, 50, 75 and 100% (v/v) in water) was introduced in the centre of each drawn shape, to see whether it would stay within the borders.

2.6. Preconcentration for paper microfluidics and PSI

Preconcentration of reagents was achieved on paper by drawing hexagonal grids and employing the selective permeability feature of AKD barriers [26]. A volume of 3 μL of water-based dye was carefully pipetted into each hexagon and allowed to dry. To elute the dried dyes, a solution of 50% (v/v) methanol in water was used.

The ink was also used to preconcentrate sample on a paper-spray ionization tip to enhance the sensitivity of the signal detection of PSI-MS. For this application, the ink was diluted 1:1 with water, applied to the paper tip and heated in an oven at 100 °C for 15 min. This higher temperature was chosen for heating the AKD in this case to ensure that the AKD reacted as completely as possible with the cellulose, to prevent unreacted AKD from eluting and causing interfering MS signal. The setup for the PSI-MS experiment (ESI Fig. S3) was developed in previous work [39,40]. In short, a paper tip for PSI needs to have a sharp tip to generate a high electrical field when a potential is applied. The sample is deposited onto the tip and allowed to dry. The sample is then eluted from the paper tip with solvent (methanol with 1% formic acid) and sprayed into the MS. In order to obtain better control over solvent distribution, spray time, focusing and desolvation of the ion spray, the tip is integrated into a functionalized, 3D-printed cartridge. The cartridge is positioned in front of the MS (API 2000, Sciex) on a 3D-printed holder. More details about the operating parameters can be found in the previous publications [39,41], as well as in a summary in Table S3 of the ESI.

For this report, the paper tip was either used as it was (unpatterned), or after patterning it with diluted AKD ink. For the latter, a straight line was hand-drawn across the tip close to its end using the plotter pen, after which the paper tip was heated in an oven as described above in this section. Afterwards, the tip was suspended in three successive aliquots of fresh methanol for 10 min each to wash it, after which it was dried. Five μL of an aqueous solution of methylene blue (20 μM) and crystal violet (20 μM) was pipetted onto the ends of both patterned and unpatterned paper spray tips and allowed to dry. The paper was then loaded into a 3D-printed cartridge, positioned in front of the orifice of the MS and used to generate ion spray from which the analytes could be detected.

3. Results and discussion

3.1. Formulation of AKD ink

To produce AKD particles suspended in water, an emulsion of a chloroform solution of AKD in water needs to be made first. The conical flask containing the emulsion is immersed in a 60 °C water bath. The chloroform droplets will thus decrease in size as chloroform evaporates due to the heat provided by the water bath. Eventually, the chloroform is mostly removed and a cooling step is executed, yielding a suspension of fine AKD particles in water. Assuming that the AKD content of each chloroform droplet will produce an AKD particle, it becomes clear that emulsion properties are crucial for ensuring the size uniformity of the particles produced. Particles with small size (<10 μm) and a narrow size distribution are preferred for three reasons:

(i) The size of the particles should be small enough to avoid clogging the patterning tools during use, in this case the plotter pen or the DIY pen.
(ii) Particle size should be small enough to reduce sedimentation and aggregation in the flask while on the shelf. It was observed that small, uniformly sized particles produced a dispersion that was stable for a few hours (ESI Fig. S4). After sedimentation, the AKD particles can be redispersed by gentle swirling.
(iii) Particle uniformity affects the quality of the patterns produced on paper upon heating. AKD ink is wicked into the paper by capillary action, with AKD particles traveling with

the dispersing medium. These are then retained somewhere within the pores, depending on the particle size. Large particles tend to be retained closer to the paper surface and produce a broader line pattern at the surface as a result, while small particles penetrate deeper into the pores and produce a more uniform line pattern.

We used image analysis to estimate the size distribution of the suspensions, as detailed in ESI Protocol S1. More accurate methods exist for estimating particle size distributions in a suspension. However, this method was selected because it allowed us to rapidly assess whether particle sizes were small enough to avoid the above-mentioned concerns.

3.1.1. Surfactant

The type of surfactant and surfactant concentration are critical parameters in producing small, uniformly sized particles for AKD ink. When we tried to produce the ink from a chloroform-water mixture in the absence of surfactant, a two-layer system was obtained. Furthermore, at the end of the procedure, AKD particles with a broad size distribution, including anomalously large particles, were observed in the flask. Fig. 2A demonstrates the effect of surfactant on the AKD particle size in the final product.

At all concentration levels of T20, both small and large particles were observed, indicating that the emulsions formed are not very stable. As a result, a substantial number of visibly larger AKD particles could be observed in the final suspension (ESI Fig. S5).

The violin plot in Fig. 2A shows that TTAB yields a narrower distribution of particle sizes than T20, with a maximum diameter of 17 μm as compared to 65 μm for T20, excluding a few much larger "chunks". For TTAB 10x and 20x, the largest population is attributed to particles of 1−2 μm, with 75% of the total population below 6 μm. The range of sizes represented by these two conditions is suitable for pens having an orifice of 20 μm or larger. The ink produced under these two conditions did not cause any clogging during the patterning step, and pens were easy to clean by rinsing with water at room temperature.

On the other hand, TTAB 2x was insufficient to form a stable emulsion. Most of the AKD adhered to the magnetic stir bar during the mixing. As a result, only a small number of AKD particles were present in the final suspension. Thus, a substantially smaller population of particles was observed for TTAB 2x as compared to TTAB 10x and 20x. As no apparent difference was observed between TTAB 10x and 20x, TTAB 10x was chosen as the optimal surfactant concentration and used for subsequent experiments. A lower concentration of TTAB is preferred to minimize possible interference signal when AKD ink is employed to pattern paper tips for use with a sensitive detection system such as PSI-MS.

3.1.2. Route of emulsification

Fig. 2B shows the impact of the route of emulsification on particle size and size distribution. While the statistical modes (most frequently appearing value; ~1 μm) and medians (value of the middle data point/red dot in the violin plot; 2−3 μm) are comparable for all routes, we find a clear difference in the maximum particle size of the suspensions made via the different emulsification routes. By adding the water phase (10 mL) in aliquots (1 mL every 2 min) to the oil phase (1 mL) (W-O aliquot route), particles with the narrowest size distribution and the smallest diameter were produced.

The opposite route, in which the chloroform ("oil") phase (1 mL) was added in aliquots (0.1 mL every 2 min) to the water phase (10 mL) (O-W aliquot route), gave a wider range of particle sizes. The maximum particle size (29 μm) was almost double that for the W-O aliquot route (15 μm).
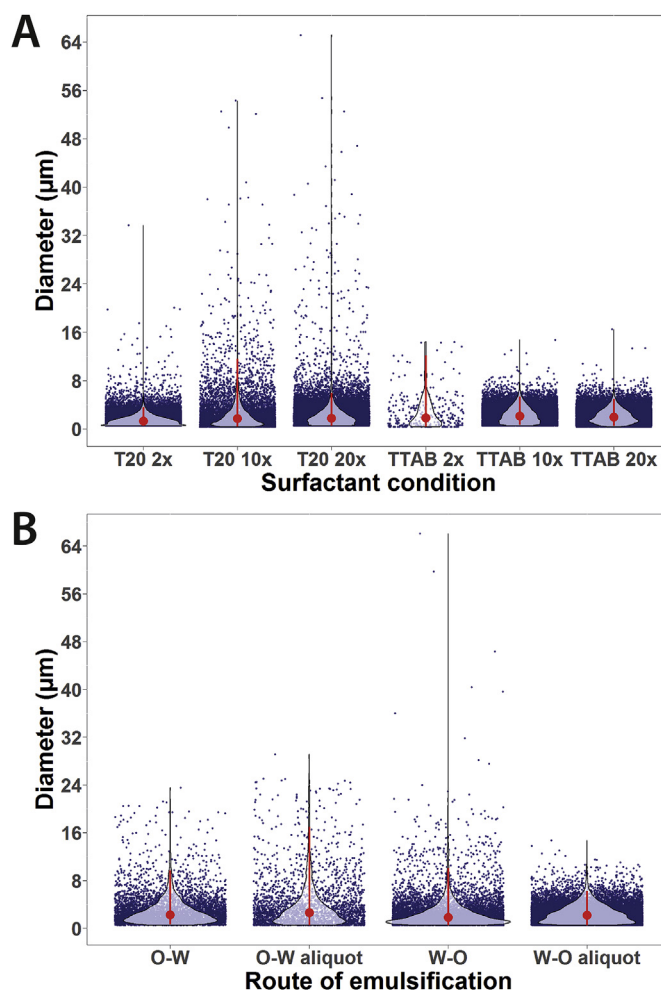
Fig. 2. The violin plots (number-based distribution) and scatter plots representing the effect of (A) surfactant conditions and (B) emulsification route on AKD particle size. The area of the violin represents the density plot with the width at a value of the y-axis being the relative frequency of particles having that particular size. The vertical red lines and dots denote the interquartile range and median (based on the 95% confidence interval), respectively. The scatter plot (blue dots) behind each violin plot represents the population of individual particles for the respective condition. Emulsification using TTAB 10x and W-O aliquot route was chosen as the optimized set of conditions. (For interpretation of the references to colour in this figure legend, the reader is referred to the web version of this article.)

Mohlin et al. demonstrated that a smaller droplet size can be achieved by adding water to a mixture of oil and surfactant, rather than the other way around. A similar trend was observed in this work even though a different surfactant system was used than by Mohlin et al. [34].

For the oil-to-water (O-W) and water-to-oil (W-O) routes, the two phases were combined in their entirety all at once. Both routes lead to a particle population in which 75% of the particles have a diameter below 10 μm. The presence of relatively large particles with the W-O route might be attributed to the fact that a large volume (10 mL) of water at room temperature was added to a small volume (1 mL) of chloroform at 60 °C, leading to non-homogeneous mixing.

The W-O aliquot route was selected as the best route to achieve satisfactory emulsification of chloroform solutions of AKD, resulting in high-quality suspensions of AKD particles in water.

3.1.3. Cooling condition

Varying the approach for cooling the emulsion did not lead to a

large difference in particle size (ESI Fig. S6). All conditions show similar medians (2 μm) and interquartile ranges. However, the cooling method selected does influence the time required for cooling. The cooling process (60 °C to 20 °C) took several minutes at room temperature, but only 1.5–2 min when using an ice bath, and about 20 s using a freezer programmed at −18 °C.

3.1.4. AKD concentration

Increasing AKD concentrations led only to increased particle populations, and not to changes in the size distribution (ESI Fig. S7). To prove this, we calculated a volume-based distribution by multiplying the volume occupied by a single particle having a given diameter with the number of particles of that diameter (Fig. 3A). The volume was calculated assuming spherical particles. The total volume of measured AKD particles strongly correlates to the initial AKD concentration (Fig. 3B; ESI Table S4).

3.1.5. Temperature

The chloroform-water emulsion formed was the same at room temperature as when the water bath at 60 °C was employed. However, after all the additions of water had been carried out, the room-temperature emulsion would still be translucent, indicating the presence of chloroform. In contrast, the emulsion at 60 °C had become transparent, leading us to conclude that almost all the chloroform had been removed by evaporation (<2%, ESI Fig. S1). The observation that 1 mL of chloroform in a flask in the 60 °C water bath took approximately 17 min to completely evaporate supports this conclusion. The evaporation of chloroform is evidently a gradual process at 60 °C, but the duration of the emulsification step is longer than 17 min. It is necessary to include the water bath in the experimental setup to make sure that a safe, virtually chloroform-free product is obtained.

Using the water bath at a higher temperature (70 °C), on the other hand, led to visibly less homogeneous suspensions.

3.1.6. Optimized ink formulation

In summary, the final ink formulation is based on an AKD concentration of 10 g L^{-1}, the use of the surfactant, TTAB, at a concentration equivalent to 10 times the CMC, and emulsification by the addition of water aliquots (10 × 1 mL) to 1 mL of chloroform under stirring (the W-O aliquot route). The conical flask in which the emulsion is made is immersed in a water bath at 60 °C. Once formed, the emulsion is cooled to room temperature in an ice bath. This optimized protocol was adopted for the paper patterning process. The data for the individual suspensions made using this protocol are shown in ESI Fig. S8. The particle distribution is similar in all repetitions, implying low batch-to-batch variability. On-shelf stability was assessed for this ink and the results are shown in ESI Fig. S4.

3.2. Patterning paper using AKD ink

3.2.1. Print quality, ease of printing

Handling of our water-based ink is easy compared to organic solvent-based solutions. Once the suspension has been formed, it does not require a fume hood for use, making it more convenient and less hazardous for the health of the end-user. Furthermore, the ink can be contained in the plastic barrel of the plotter pen or DIY pen without leaking or damaging the patterning tool.

The fact that AKD is present as fine, suspended particles rather than dissolved solutes limits the dispersion of AKD in paper due to particles being trapped within the porous cellulose network. As a result, structures with a line thickness of 1.12 mm (standard deviation, SD = 0.08, n = 20) can be drawn using the plotter pen (diameter of nib = 0.6 mm) and the XY-plotter (Fig. 4A,D). A
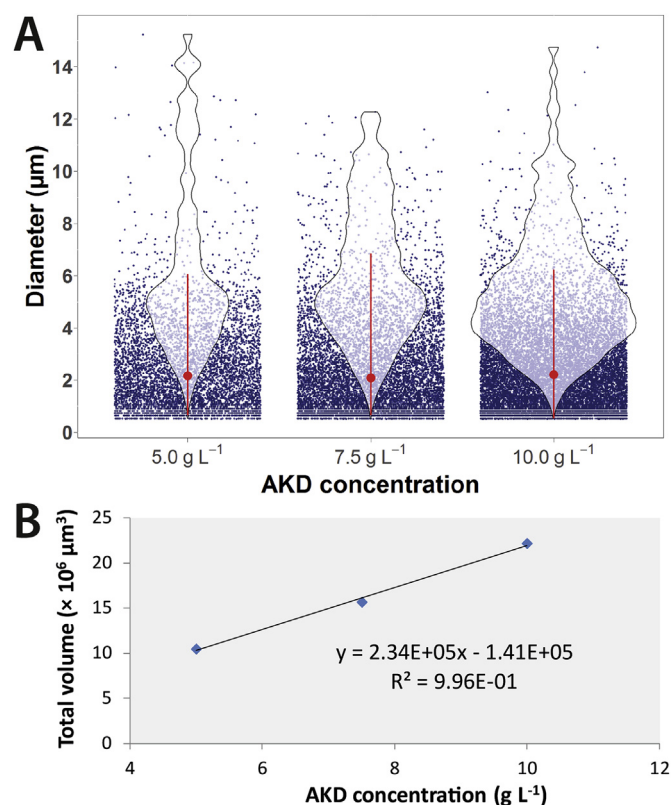

Fig. 3. Effect of AKD concentration on particle size distribution. (A) The violin plot (volume-based distribution) and scatter plot represent the effect of AKD concentration on the total volume occupied by AKD particles. Note that the median particle size is very similar for all three concentrations tested. (B) Correlation between total volume occupied by the produced particles and the AKD concentration used. These observations show that the increment in concentration only increases the population of the particles rather than affecting the size of the particles.

previously demonstrated polydimethylsiloxane (PDMS)-in-hexane ink yielded an approximate line thickness of 2.81 mm (SD = 0.30 mm) when used with a needle having a diameter of 0.6 mm and an XY-plotter [21]. This was estimated from the given figure in the reference stated using ImageJ. Hence, our AKD ink allows for a substantial improvement in line-thickness resolution compared to the previously described PDMS ink.

3.2.2. Contact angle and permeability

AKD structures were tested for their permeability with respect to water and water-methanol solutions. The hydrophobic barriers formed using the ink work well to contain water in the confined hydrophilic regions of the paper, despite the presence of surfactant in the hydrophobic barrier. In fact, aqueous solutions can be contained beyond the absorption capacity of the paper, forming droplets in the ca. 2-mm-diameter confined regions (the diameter of a single hexagon is ca. 4 mm, including the AKD walls) when relatively large volumes (3 μL) of dye solutions are deposited (Fig. 5A). When placed directly on a paper surface treated with AKD, water droplets demonstrate non-wetting behavior as evidenced by a contact angle, θ, of 135.6° (SD = 5.9; n = 3; Fig. 4F). This contact angle is higher than that found with our previously reported AKD patterning approach, which used a two-step application procedure [26]. In that work, a cellulose chromatography paper strip was first completely soaked in a 0.6 g L^{-1} AKD in hexane solution, allowed to dry, and then heated in an oven at 100 °C for 30 min. Hydrophilic channels and chambers were formed in the paper by exposing it to oxygen plasma through a stencil to remove AKD and rehydrophilize
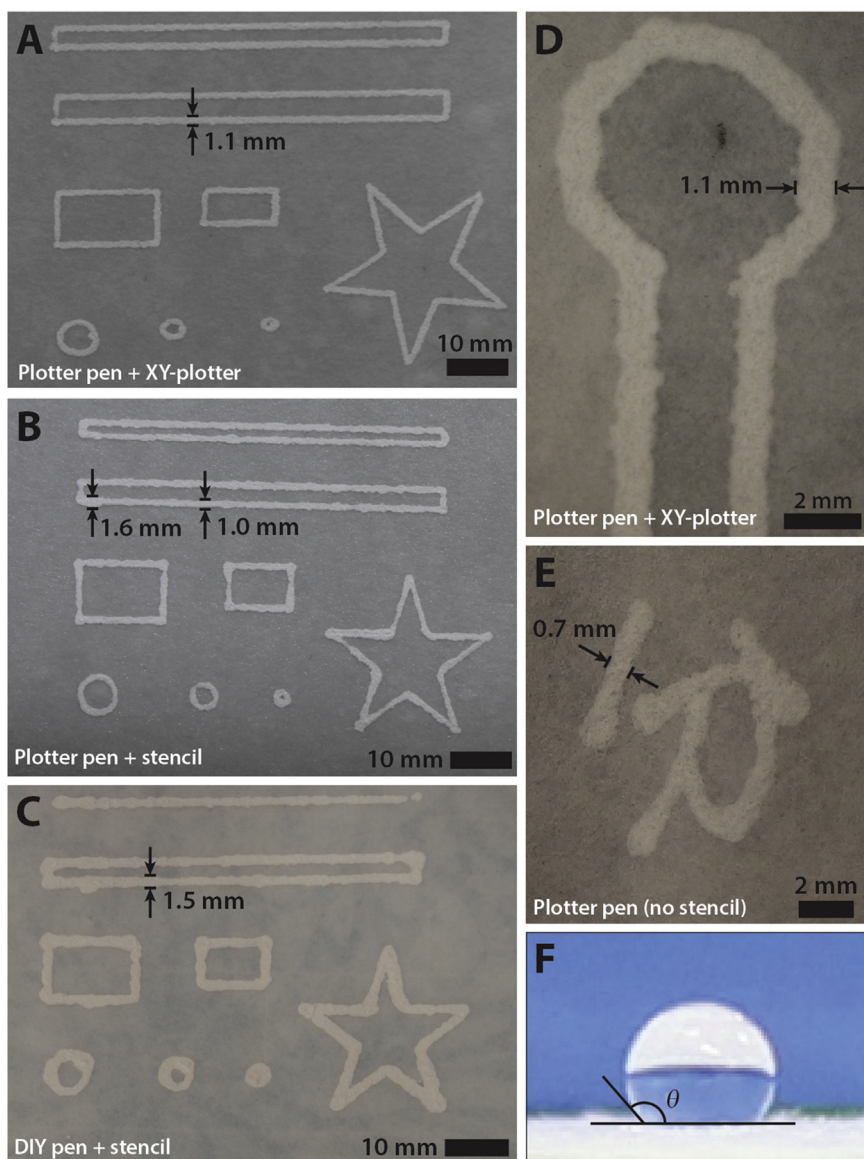
Fig. 4. A comparison of the line quality of AKD patterns produced using (A) the plotter pen in the XY-plotter, (B) the plotter pen manually with a 3D-printed stencil and (C) the stand-alone DIY pen manually with a stencil. (D) Image of a structure drawn using the plotter pen in the XY-plotter, and (E) a Chinese character drawn manually with the plotter pen (without stencil). (F) A water droplet (10 μL) on a paper surface treated with AKD ink using the plotter pen and the XY-plotter ($\theta = 135.6°$; SD = 5.9; n = 3).

the paper in these regions. A second manual application of 5 g L^{-1} AKD in hexane solution followed around the rehydrophilized regions. After a second heating step at 80 °C for 3 min, a θ of 116.5° (SD = 2.0°) was measured for aqueous droplets on that surface [26]. The higher contact-angle values recorded in this study can be attributed to the use of a higher concentration of AKD, as well as a different application method.

AKD structures in this study only remain impermeable to methanol-water mixtures containing up to 25% methanol. This methanol percentage is relatively low when compared to the AKD patterning approach described above, which allowed the confinement of 75% methanol [26]. When a large volume (ca. 30 μL) of aqueous methanol solution (>25%) was introduced into a rectangular, 11 mm × 6 mm, untreated hydrophilic region surrounded by a hydrophobic barrier, the solution started to leak through certain points in the barrier rather than wetting the whole barrier. This is probably because the distribution of AKD particles achieved by delivery of a suspension with a pen is less homogeneous than when

dipping the entire paper substrate in a hexane solution of AKD. The spreading and trapping of AKD particles within the porous network is thus less uniform than the wicking of dissolved AKD in hexane through this network, and results in the observed variable permeability of AKD barriers to solvents like methanol, which have lower surface energies than water. Moreover, barriers patterned with the aqueous particle suspension will be more permeable to solvents like methanol and solutions containing these solvents. However, patterning long and thin structures is easier using the aqueous-ink approach, and more complex structures are often as easy to draw as shapes consisting of straight lines. Additionally, the direct patterning approach reported here means that untreated hydrophilic regions remain pristine, having never come into contact with any AKD. This is a significant advantage of direct patterning when compared to our previously reported approach, in which AKD had to be removed by oxygen plasma treatment to form hydrophilic regions [26]. Finally, the present method is less laborious than the oxygen-plasma approach.
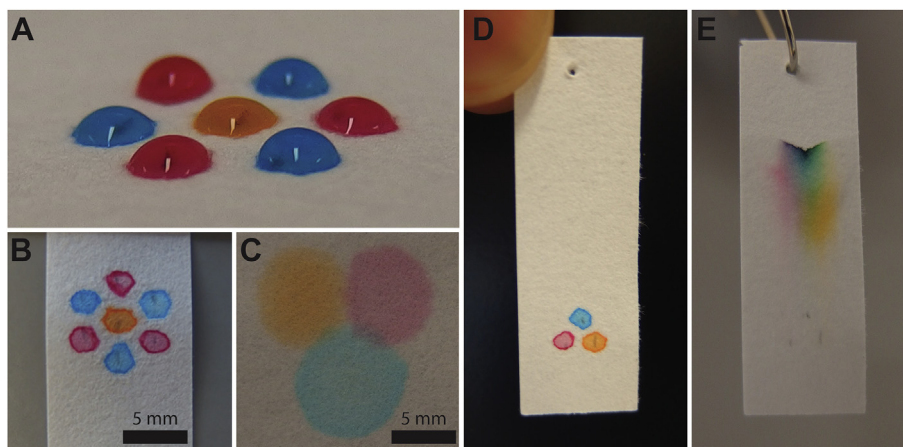
Fig. 5. Demonstration of the storage and preconcentration capabilities of small AKD-lined chambers. (A) Aqueous solutions of food dyes were pipetted into each vessel (3 μL). (B) Each dye solution was confined within the smaller area of the reagent "vessel", so that the dyes were concentrated in these areas once the water had evaporated. (C) In the absence of an AKD barrier, dyes spread out by wicking over a larger area, so that the resulting dye patches were less concentrated. Dried dye spots (D) before and (E) after elution from the hexagonal chambers by 50% methanol/50% water (v/v) solution.

3.2.3. Do-it-yourself tool for patterning with AKD ink

To test the applicability of our ink for manual patterning, the performance of the commercially acquired plotter pen and a DIY pen made from inexpensive, readily available components in the lab were compared.

In our experience, the stand-alone plotter pen used manually (without stencil) produced lines with better uniformity and a smaller width than when it was used in conjunction with the XY-plotter (Fig. 4D,E). While this result might be surprising, the pressure of the pen tip on the paper is actually better controlled by hand than with the XY-plotter. Less scratching of the paper by the tip is observed as a result. The movement of the tip becomes faster, thus producing thinner and more uniform lines. However, the quality of the patterns might vary from one user to the next. When the plotter pen was used to make patterns with a stencil, a slight variability in thickness was constantly observed (Fig. 4B). Scratching of the paper may have contributed to this variability, as well as the occasional wetting of the stencils themselves by ink when the pen tip was drawn along stencil openings.

For the DIY pen, liquid flow was influenced by the lowered surface tension of the dispersing medium (water containing surfactant) on the inner surface of the syringe needle. A volume of 500 μL of AKD was contained without leaking when a sufficiently small syringe needle (outer diameter = 0.3 mm) was used. When larger volumes were introduced to the DIY pen, the surface tension was overcome by the higher hydrostatic pressure, and leaking was observed. Using syringe needles with larger diameters also resulted in leakage of ink.

The flow of ink was more difficult to control with the DIY pen than with the plotter pen (Fig. 4C). Nevertheless, the larger variation in thickness did not adversely affect the observed impermeability to water of the produced hydrophobic structures. For patterning small structures, it is recommended to use tools or equipment which provide better control of ink flow, such as that offered by the plotter pen.

3.3. Reagent storage and preconcentration

3.3.1. Reagent storage for paper microfluidics

Because of the wicking of liquid through paper, even a small volume of reagents will be smeared out over a relatively large area when spotted on untreated paper. To overcome the spreading of sample, smaller aliquots of liquid need to be spotted and dried repeatedly, as commonly practiced in paper chromatography and thin-layer chromatography. This ultimately limits the number of reagents that can be stored separately (e.g. to avoid unwanted pre-assay reactions) within a small area of a paper device.

By exploiting the selective permeability characteristics of AKD patterned paper [26], small "vessels" of reagents can be created by simply drawing small, closed structures on paper (Fig. 5A). Deposited reagent will be confined within these structures and become concentrated as the solvent dries off (Fig. 5B). Because relatively thin lines of barrier can be drawn, a large number of vessels can be arranged close together according to device requirements. This is advantageous over the conventional way of applying reagents on paper, in which the reagents wick out over a large area of the paper and become diluted (Fig. 5C). When needed, the reagents can be released by eluting them from their chambers with an aqueous solution of methanol at 50% (v/v) or higher (Fig. 5D–E).

3.3.2. Preconcentration for PSI

We further utilized this selective permeability feature for sample preconcentration for PSI-MS, to improve the elution efficiency and signal intensity of compounds with relatively high retention on paper. This ionization technique is based on the generation of a continuous spray of solvent containing analytes, crystal violet and methylene blue in this case, from a paper tip into the MS with the help of a high potential. As the solvent spray approaches the MS, solvent evaporates, resulting in liberated gas-phase ions which can be detected by the MS [36].

Fig. 6A, and B shows a schematic and a photograph of unpatterned paper tips. When analyte is spotted onto such a tip and is eluted toward the sharp extremity, the analyte band automatically becomes more focused due to the converging geometry. The latter is mainly true for molecules which have only weak retention on paper, and can thus be concentrated by simple elution. However, this effect is less pronounced for analytes that are retained more strongly on paper. Fig. 6C and D demonstrate that the signal of a relatively strongly-retained analyte, methylene blue, appeared much slower and weaker in the mass spectra compared to an easily-eluted analyte, crystal violet.

To improve the signal of slowly eluting compounds, they can be focused on the front-most part of the tip during the deposition step. To achieve this, a simple line of AKD was patterned close to the sharp tip of the paper using the plotter pen to limit the spreading of
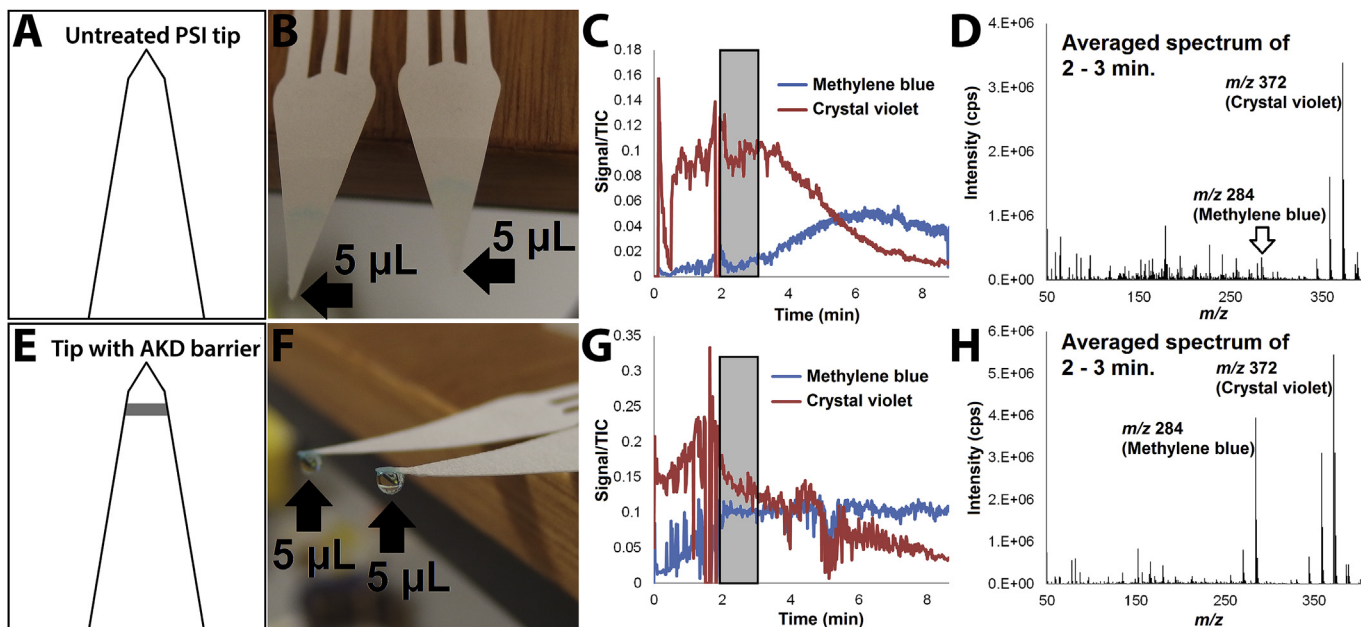
Fig. 6. Comparison of the behavior of (A–D) an untreated and (E–H) an AKD-patterned paper tip for PSI. (A–B) The unmodified tip simply consists of a porous cellulose network, so when aqueous sample is introduced at the front (indicated by arrows), the liquid wicks into the tip. Analyte is smeared out over an area extending back from the tip, with low local concentrations as a result. (E–F) The tips in this case have been patterned with AKD ink by drawing a line across the tip to define a small confined region at the front end, which is separated from the rest of the tip by the AKD barrier. When the same aqueous sample volume is applied to one of these patterned tips, a droplet is formed at the front end, and analyte is preconcentrated in this region once the solvent has evaporated. In order to demonstrate the sample preconcentration effect of this patterning approach, an aqueous mixture of crystal violet (20 μM) and methylene blue (20 μM) was selected for a PSI-MS experiment. Methanol containing 1% formic acid was chosen as spray solvent. Crystal violet elutes readily with methanol, and therefore is focused upon elution. However, methylene blue shows stronger retention and therefore experiences little focusing. This is reflected in the relative MS traces over time (related to the total ion current). In data obtained for an unpatterned tip (C), we observe a strong initial signal for crystal violet and a low signal for methylene blue; the latter slowly increases over time on unpatterned paper. In contrast, in the MS trace in (G), obtained for a patterned tip, the methylene blue signal is initially much stronger due to sample preconcentration, leading to faster and more efficient elution. This is even clearer in the averaged spectrum between 2 and 3 min of spraying, in which we see (D) little signal for methylene blue and high signal for crystal violet, while (H) on a treated paper tip, the signals are much more comparable in intensity. (For interpretation of the references to colour in this figure legend, the reader is referred to the web version of this article.)

a solution pipetted at the tip (Fig. 6E,F), which works in a manner very similar to the reagent vessels discussed above. As a result, the elution of methylene blue began earlier and more efficiently (Fig. 6G,H) as compared to the paper tip without AKD pattern. The MS signal for methylene blue increased 10-fold as early as t = 2 min, due to the pre-concentrating effect of the selectively permeable barrier. It increased with respect to the signal for crystal violet as well, indicating that the concentration effect is stronger for methylene blue than for crystal violet. The latter makes perfect sense, since the weakly retained crystal violet is normally already concentrated upon elution. Hence, the effect of additional pre-concentration through confinement of sample deposition to the very end of the tip is less pronounced for this compound than for the more strongly retained methylene blue, a compound that experiences very little concentration effect during elution.

4. Conclusion

We have demonstrated the development and implementation of a novel AKD ink for hydrophobic patterning of paper. This work differs significantly from previously reported ink, for the following three reasons. First, we have developed an AKD patterning agent based on water instead of the organic solvent, heptane, a solvent known to be hazardous to human health. This has major implications for the safe implementation of our ink outside of standard lab settings, as the need for a fumehood for paper patterning is circumvented. A water-based AKD ink also does not damage plastic-based tools or equipment, making it more flexible in its use.

Second, the ink can be applied manually onto paper (very

inexpensive, and also permits application to irregularly shaped paper devices), or in an automated fashion with e.g. a 2D plotter (for higher production rate and reproducibility). This is fundamentally different from previously published applications utilizing an inkjet printer, which (i) require technical modification of the hardware, (ii) can only be used in a stationary setup, without possibilities of patterning anything other than a standard-format, flat sheet of paper, and (iii) is significantly more expensive in its acquisition and use than a simple (plotter) pen.

Third, we show for the first time that AKD patterns can be used not only to pattern paper and confine fluids, but also to pre-concentrate sample through confinement to a small area and subsequent evaporation of the solvent. Since AKD patterns are selectively permeable, preconcentrated sample can easily be retrieved by elution using a different solvent system known to breach AKD patterns.

We have further demonstrated the applicability of the new aqueous ink in a PSI-MS experiment, in which the signal intensity of especially those compounds which elute slowly (are more retained) was increased through incorporation of a selectively permeable AKD barrier towards the front end of the tip.

The resolution of the patterns drawn using the ink and an XY-plotter are on the order of 1 mm using a plotter with a 0.6 mm nib. The resolution offered by conventional wax printers is slightly better, with line thicknesses on the order of 0.85 mm [22], due to better control of wax droplet deposition. However, the proposed technique in this work offers more flexibility for on-site device modification, as well as general handling.

We believe that this ink and the patterning tools used are

effective options for the fabrication of multifunctional paper microfluidic tools, both in and for low-resource settings. AKD-patterned paper devices will contribute towards solving analytical challenges in application fields such as environmental analysis and point-of-care diagnostics.

Author contributions

All authors contributed significantly to the creation of this manuscript. All authors have given approval for the final version of the manuscript.

Acknowledgements

Appendix A. Supplementary data

Supplementary data related to this article (in which referred as the Electronic Supplementary Information, ESI) can be found at https://doi.org/10.1016/j.aca.2017.10.040.

References

[1] E.W. Washburn, The dynamics of capillary flow, Phys. Rev. 17 (1921) 273—283, https://doi.org/10.1103/PhysRev.17.273.

[2] R. Masoodi, K.M. Pillai, Darcy's law-based model for wicking in paper-like swelling porous media, AIChE J. 56 (2010) 2257—2267, https://doi.org/10.1002/aic.12163.

[3] A.T. Jafry, H. Lim, S. Il Kang, J.W. Suk, J. Lee, A comparative study of paper-based microfluidic devices with respect to channel geometry, Colloids Surfaces A Physicochem. Eng. Asp. 492 (2016) 190—198, https://doi.org/10.1016/j.colsurfa.2015.12.033.

[4] A.W. Martinez, S.T. Phillips, M.J. Butte, G.M. Whitesides, Patterned paper as a platform for inexpensive, low-volume, portable bioassays, Angew. Chem. Int. Ed. Engl. 46 (2007) 1318—1320, https://doi.org/10.1002/anie.200603817.

[5] E. Fu, S.A. Ramsey, P. Kauffman, B. Lutz, P. Yager, Transport in two-dimensional paper networks, Nanofluid. Nanofluidics 10 (2011) 29—35, https://doi.org/10.1007/s10404-010-0643-y.

[6] A.K. Yetisen, M.S. Akram, C.R. Lowe, Paper-based microfluidic point-of-care diagnostic devices, Lab. Chip 13 (2013) 2210—2251, https://doi.org/10.1039/c3lc50169h.

[7] K.F. Lei, C.-H. Huang, R.-L. Kuo, C.-K. Chang, K.-F. Chen, K.-C. Tsao, N.-M. Tsang, Paper-based enzyme-free immunoassay for rapid detection and subtyping of influenza A H1N1 and H3N2 viruses, Anal. Chim. Acta 883 (2015) 37—44, https://doi.org/10.1016/j.aca.2015.02.071.

[8] D.M. Cate, W. Dungchai, J.C. Cunningham, J. Volckens, C.S. Henry, Simple, distance-based measurement for paper analytical devices, Lab. Chip 13 (2013) 2397—2404, https://doi.org/10.1039/c3lc50072a.

[9] E. Carrilho, S.T. Phillips, S.J. Vella, A.W. Martinez, G.M. Whitesides, Paper microzone plates, Anal. Chem. 81 (2009) 5990—5998, https://doi.org/10.1021/ac900847g.

[10] R. Dey, S. Kar, S. Joshi, T.K. Maiti, S. Chakraborty, Ultra-low-cost "paper-and-pencil" device for electrically controlled micromixing of analytes, Microfluid. Nanofluidics (2015) 375—383, https://doi.org/10.1007/s10404-015-1567-3.

[11] J.L. Osborn, B. Lutz, E. Fu, P. Kauffman, D.Y. Stevens, P. Yager, Microfluidics without pumps: reinventing the T-sensor and H-filter in paper networks, Lab. Chip 10 (2010) 2659—2665, https://doi.org/10.1039/c004821f.

[12] Z.W. Zhong, R.G. Wu, Z.P. Wang, H.L. Tan, An investigation of paper based microfluidic devices for size based separation and extraction applications, J. Chromatogr. B 1000 (2015) 41—48, https://doi.org/10.1016/j.jchromb.2015.07.010.

[13] T. Songjaroen, W. Dungchai, O. Chailapakul, C.S. Henry, W. Laiwattanapaisal, Blood separation on microfluidic paper-based analytical devices, Lab. Chip 12 (2012) 3392—3398, https://doi.org/10.1039/c2lc21299d.

[14] X. Yang, O. Forouzan, T.P. Brown, S.S. Shevkoplyas, Integrated separation of blood plasma from whole blood for microfluidic paper-based analytical devices, Lab. Chip 12 (2012) 274—280, https://doi.org/10.1039/c1lc20803a.

[15] N.R. Pollock, J.P. Rolland, S. Kumar, P.D. Beattie, S. Jain, F. Noubary, V.L. Wong, R.A. Pohlmann, U.S. Ryan, G.M. Whitesides, A paper-based multiplexed transaminase test for low-cost, point-of-care liver function testing, Sci. Transl. Med. Sept. 19 (2012), https://doi.org/10.1126/scitranslmed.3003981, 152—129.

[16] N.R. Pollock, S. McGray, D.J. Colby, F. Noubary, H. Nguyen, T.A. Nguyen, S. Khormaee, S. Jain, K. Hawkins, S. Kumar, J.P. Rolland, P.D. Beattie, N.V. Chau, V.M. Quang, C. Barfield, K. Tietje, M. Steele, B.H. Weigl, Field evaluation of a prototype paper-based point-of-care fingerstick transaminase test, PLoS One 8 (2013) 1—10, https://doi.org/10.1371/journal.pone.0075616.

[17] S.A. Bhakta, R. Borba, M. Taba, C.D. Garcia, E. Carrilho, Determination of nitrite in saliva using microfluidic paper-based analytical devices, Anal. Chim. Acta 809 (2014) 117—122, https://doi.org/10.1016/j.aca.2013.11.044.

[18] X. Chen, J. Chen, F. Wang, X. Xiang, M. Luo, X. Ji, Z. He, Determination of glucose and uric acid with bienzyme colorimetry on microfluidic paper-based analysis devices, Biosens. Bioelectron. 35 (2012) 363—368, https://doi.org/10.1016/j.bios.2012.03.018.

[19] S.M. Zakir Hossain, R.E. Luckham, A.M. Smith, J.M. Lebert, L.M. Davies, R.H. Pelton, C.D.M. Filipe, J.D. Brennan, Development of a bioactive paper sensor for detection of neurotoxins using piezoelectric inkjet printing of sol-gel-derived bioinks, Anal. Chem. 81 (2009) 5474—5483, https://doi.org/10.1021/ac900660p.

[20] R.S.J. Alkasir, M. Ornatska, S. Andreescu, Colorimetric paper bioassay for the detection of phenolic compounds, Anal. Chem. 84 (2012) 9729—9737, https://doi.org/10.1021/ac301110d.

[21] D.A. Bruzewicz, M. Reches, G.M. Whitesides, Low-cost printing of poly(dimethylsiloxane) barriers to define microchannels in paper, Anal. Chem. 80 (2008) 3387—3392, https://doi.org/10.1021/ac702605a.

[22] E. Carrilho, A.W. Martinez, G.M. Whitesides, Understanding wax printing: a simple micropatterning process for paper-based microfluidics, Anal. Chem. 81 (2009) 7091—7095, https://doi.org/10.1021/ac901071p.

[23] X. Li, J. Tian, T. Nguyen, W. Shen, Paper-based microfluidic devices by plasma treatment, Anal. Chem. 80 (2008) 9131—9134, https://doi.org/10.1021/ac801729t.

[24] B. Lutz, T. Liang, E. Fu, S. Ramachandran, P. Kauffman, P. Yager, Dissolvable fluidic time delays for programming multi-step assays in instrument-free paper diagnostics, Lab. Chip 13 (2013) 2840—2847, https://doi.org/10.1039/c3lc50178g.

[25] J. Houghtaling, T. Liang, G. Thiessen, E. Fu, Dissolvable bridges for manipulating fluid volumes in paper networks, Anal. Chem. 85 (2013) 11201—11204, https://doi.org/10.1021/ac4022677.

[26] G.IJ. Salentijn, N.N. Hamidon, E. Verpoorte, Solvent-dependent on/off valving using selectively permeable barriers in paper microfluidics, Lab. Chip 16 (2016) 1013—1021, https://doi.org/10.1039/C5LC01355K.

[27] X. Li, J. Tian, G. Garnier, W. Shen, Fabrication of paper-based microfluidic sensors by printing, Colloids Surf. B. Biointerfaces 76 (2010) 564—570, https://doi.org/10.1016/j.colsurfb.2009.12.023.

[28] K.L. Dornelas, N. Dossi, E. Piccin, A simple method for patterning poly(dimethylsiloxane) barriers in paper using contact-printing with low-cost rubber stamps, Anal. Chim. Acta 858 (2015) 82—90, https://doi.org/10.1016/j.aca.2014.11.025.

[29] K. Abe, K. Kotera, K. Suzuki, D. Citterio, Inkjet-printed paperfluidic immuno-chemical sensing device, Anal. Bioanal. Chem. 398 (2010) 885—893, https://doi.org/10.1007/s00216-010-4011-2.

[30] K. Abe, K. Suzuki, D. Citterio, Inkjet-printed microfluidic multianalyte chemical sensing paper, Anal. Chem. 80 (2008) 6928—6934, https://doi.org/10.1021/ac800604v.

[31] H. Yang, Q. Kong, S. Wang, J. Xu, Z. Bian, X. Zheng, C. Ma, S. Ge, J. Yu, Hand-drawn&written pen-on-paper electrochemiluminescence immunodevice powered by rechargeable battery for low-cost point-of-care testing, Biosens. Bioelectron. 61 (2014) 21—27, https://doi.org/10.1016/j.bios.2014.04.051.

[32] A. Määttänen, D. Fors, S. Wang, D. Valtakari, P. Ihalainen, J. Peltonen, Paper-based planar reaction arrays for printed diagnostics, Sensors Actuators B Chem. 160 (2011) 1404—1412, https://doi.org/10.1016/j.snb.2011.09.086.

[33] G. Garnier, J. Wright, L. Godbout, L. Yu, Wetting mechanism of alkyl ketene dimers on cellulose films, Colloid. Surface. Physicochem. Eng. Aspect. 145 (1998) 153—165, https://doi.org/10.1016/S0927-7757(98)00668-2.

[34] K. Mohlin, K. Holmberg, J. Esquena, C. Solans, Study of low energy emulsification of alkyl ketene dimer related to the phase behavior of the system, Colloid. Surface. Physicochem. Eng. Aspect. 218 (2003) 189—200, https://doi.org/10.1016/S0927-7757(02)00585-X.

[35] T. Lindstrom, P.T. Larsson, Alkyl ketene dimer (AKD) sizing - a review, Nord. Pulp Pap. Res. J. 23 (2008) 202—209, https://doi.org/10.3183/NPPRJ-2008-23-02-p202-209.

[36] J. Liu, H. Wang, N.E. Manicke, J.-M. Lin, R.G. Cooks, Z. Ouyang, Development, characterization, and application of paper spray ionization, Anal. Chem. 82

(2010) 2463–2471, https://doi.org/10.1021/ac902854g.

[37] K. Missoum, F. Martoïa, M.N. Belgacem, J. Bras, Effect of chemically modified nanofibrillated cellulose addition on the properties of fiber-based materials, Ind. Crops Prod. 48 (2013) 98–105, https://doi.org/10.1016/j.indcrop.2013.04.013.

[38] C.A. Schneider, W.S. Rasband, K.W. Eliceiri, NIH Image to ImageJ: 25 years of image analysis, Nat. Methods 9 (2012) 671–675, https://doi.org/10.1038/nmeth.2089.

[39] G.IJ. Salentijn, H.P. Permentier, E. Verpoorte, 3D-printed paper spray

ionization cartridge with fast wetting and continuous solvent supply features, Anal. Chem. 86 (2014) 11657–11665, https://doi.org/10.1021/ac502785j.

[40] G.I.J. Salentijn, R.D. Oleschuk, E. Verpoorte, 3D-printed paper spray ionization cartridge with integrated desolvation feature and ion optics, Anal. Chem. 89 (2017) 11419–11426, https://doi.org/10.1021/acs.analchem.7b02490.

[41] G.IJ. Salentijn, N.N. Hamidon, E. Verpoorte, Sample preconcentration for paper spray ionization with a selectively permeable valve, in: 20th Int. Conf. Miniaturized Syst. Chem. Life Sci., Dublin, 2016, pp. 1308–1309.